Macromolecules

Article

pubs.acs.org/Macromolecules

Impact of Backbone Rigidity on the Photomechanical Response of Glassy, Azobenzene-Functionalized Polyimides

David H. Wang, Jeong Jae Wie, Kyung Min Lee, Timothy J. White,* and Loon-Seng Tan*

Air Force Research Laboratory, Materials & Manufacturing Directorate, Wright-Patterson Air Force Base, Ohio 45433-7750, United States

Supporting Information

ABSTRACT: Azobenzene-functionalized polyimide materials can directly transduce light into mechanical force. Here, we examine the impact of polymer backbone rigidity on the photomechanical response in a series of linear, azobenzene-functionalized polymers. The rigidity of the backbone was varied by the polymerization of five dianhydride monomers with a newly synthesized diamine (azoBPA-diamine). The azobenzene-functionalized linear polymers exhibit glass transition temperatures (T_g) ranging from 276 to 307 °C and maintain excellent thermal stability. The photomechanical response of these materials was characterized by photoinduced cantilever bending as well as direct measurement of photogenerated stress upon exposure to linearly polarized, 445 nm light. Increasing the rigidity of the polymer backbone increases the magnitude of stress that is generated but decreases the angle of cantilever deflection.

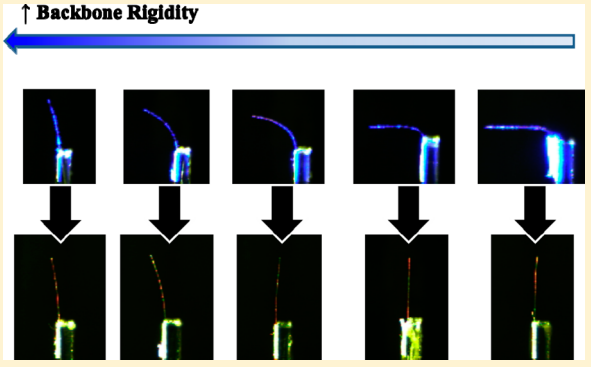

INTRODUCTION

Photomechanical effects in polymers have been pursued for nearly 50 years.[1] Photoinitiated shape adaptivity or force generation (actuation) are particularly intriguing due to the salient features of light: remote and wireless (contactless) triggering with ease of spatial, temporal, directional (through polarization), and magnitude (with intensity) control. Much of the recent literature has focused on the preparation and characterization of azobenzene-functionalized liquid crystalline polymer networks (azo-LCNs). Azo-LCNs are distinguished in that the local director orientation can be manipulated to generate monolithic, engineered materials ultimately designed for a particular shape or surface response.[2−4] However, higher performance materials such as polyimides may be advantageous, particularly in applications of the materials in load-bearing or extreme environments.[5−8]

Polyimides represent an important class of heat-resistant polymers useful in a variety of applications deriving from their excellent combination of physical properties, thermal stability, and processability.[9−11] Azobenzene-functionalized polyimides have been investigated for photoinduced alignment of liquid crystal devices and nonlinear optical (NLO) materials.[12−16] Recent examinations from our groups[5−8,17] have extended upon the work of Agolini and Gay[18] in studying photomechanical effects in azobenzene-functionalized polyimides (azo-PIs). Photomechanical effects based on azobenzene and other photochemical units and processes have also been subject to considerable recent attention in polymeric[19−21] as well as crystalline materials.[22−24]

We have reported that up to 1.3 MPa of stress can be wirelessly photogenerated in azobenzene-functionalized polyimide materials. The two order of magnitude improvement (compared to azo-LCNs of similar azobenzene concentration) is attributable to the high performance characteristics of polyimides. Our prior work has primarily focused on the characterization of cross-linked azobenzene-containing aromatic polyimides and investigated the influence of structural and morphological factors on the photomechanical response of these materials.[5−8,17] Subsequent to this initial report, we have reported on enhancement of photogenerated stress by prestraining (hot drawing),[7] polarization-controlled flexural−torsional (bend and twist) deflections,[8] and the role of free volume on the resulting photomechanical response.[17] We have also recently reported on the preparation and characterization of linear polyimide materials containing main-chain azobenzene units.[5] Through systematic preparation of (co)polyimides prepared from flexible (6FDA) and rigid (PMDA) dianhydrides and a structurally rigid diamine (4,4′-diaminoazobenzene) we have shown that crystallinity decreases the magnitude of bending and photogenerated stress.[25]

A number of recent reports have theoretically examined photomechanical effects in both liquid crystalline[26−31] and amorphous[32−34] polymers. Of relevance to the work presented here, Toshchevikov et al.[32−34] correlate descriptors of the local macromolecular environment (such as the Kuhn segment and chromophore number density) to the resulting photomechanical output. The goal of this work is to experimentally elucidate the contribution of the backbone rigidity of a series of

Received: October 22, 2013
Revised: December 30, 2013
Published: January 13, 2014

amorphous linear polyimides to the photomechanical output. Toward this end, we synthesized a new, bis(azobenzene)-diamine monomer and used it to prepare five, amorphous azobenzene-functionalized linear polyimides through polymerization with structurally distinctive dianhydride monomers. The thermal and optical properties of the materials were characterized with dynamic mechanical analysis, differential scanning calorimetry, thermogravimetric analysis, X-ray, and UV−vis spectroscopy while the photomechanical response was visualized with cantilever bending and measured in a tensile experiment. Understanding the impact of the local molecular environment on photomechanical output provides information critical to enabling the continued optimization and development of the materials chemistry to improve the effectiveness and efficiency of these materials as energy transducers.

EXPERIMENTAL SECTION

Materials. 1,3-Bis(3-aminophenoxy)benzene (ABP) (99% min.), pyromellitic dianhydride (PMDA), 3,3′,4,4′-biphenyltetracarboxylic dianhydride (BPDA), 3,3′,4,4′-benzophenonetetracarboxylic dianhydride (BTDA), and oxy-4,4′-di(phthalic anhydride) (ODPA) were purchased from Chriskev Company, Inc. 1,1,1,3,3,3-Hexafluoro-2,2-bis(4-phthalic anhydride)propane (6FDA) was purchased from Akron Polymer Systems. All five dianhydrides were sublimed before use. All other reagents and solvents were purchased from Aldrich Chemical Inc. and used as received, unless otherwise noted.

Instrumentation. The mechanical properties and photogenerated stress of polyimide films (6 mm (L) × 2 mm (W) × 0.02 mm (T)) were measured by a strain-controlled dynamic mechanical analyzer (DMA, TA Instruments RSA III) in tension. In a transient mode, stress−strain curves were obtained with a 0.01 s^{-1} Hencky strain (or true strain) rate, and tensile modulus was determined from logarithmic modulus−strain plots by extrapolating the modulus plateau to zero strain. The glass transition temperatures of the polyimides are reported from the maximum tan δ (loss modulus/storage modulus) by a stress-controlled DMA (TA Instruments DMA Q800) with a heating rate of 4 °C/min in a nitrogen atmosphere. Infrared (IR) spectra were recorded on a Nicolet Nexus 470 spectrometer, and attenuated total reflectance IR (ATR-IR) spectra were collected on a Bruker Alpha-R spectrometer. Proton and carbon nuclear magnetic resonance (NMR) spectra were measured at 300 MHz with a Bruker AVANCE 300 spectrometer. Thermogravimetric analysis (TGA) was conducted in either nitrogen (N_2) or air atmosphere at a heating rate of 10 °C/min using a TA Hi-Res TGA 2950 thermogravimetric analyzer. Gas chromatography/mass spectroscopy (GC/MS) was then performed using a Varian 1200 Series. Melting points were obtained from Buchi melting point apparatus B-545 with a heating rate of 2 °C/min. Wide-angle X-ray experiments were carried out on a Statton box camera at 53 mm sample-to-image plate distances in transmission mode using Cu Kα generated by a Rigaku Ultrax18 system.

Photomechanical effects in the polyimide materials were characterized with irradiation of linearly polarized 445 nm light at room temperature. All measurements were conducted with light polarization parallel to long axis of the cantilevers ($E\|x$). The cantilever dimensions were 6 mm (L) × 0.1 mm (W) × 0.02 mm (T) for all the experiments reported here. Photogenerated stress was measured upon illumination with linearly polarized ($E\|x$) blue light from a 445 nm light-emitting diode (LED) to polyimide films held in DMA at minimal prestrain (4×10^{-5}%). Time-resolved evolution of both cantilever bending and photogenerated stress were monitored with light exposure for 1 h.

UV−vis absorption spectra of spin-coated polyimide were captured by a Cary 5000 UV−vis−NIR spectrometer. The time-dependent absorbance of the polyimides was monitored for 1 h upon exposure to linearly polarized ($E\|x$) 445 nm light at 60 mW/cm^2.

2,2-Bis[4-(4-nitrophenoxy)phenyl]propane (3). Into a 1 L three-necked flask equipped with a magnetic stir bar and nitrogen inlet and outlet were placed 2,2-bis(4-hydroxyphenyl)propane (**1**; 18.0 g, 79.0 mmol), 4-fluoronitrobenzene (**2**; 25.0 g, 180 mmol), potassium carbonate (24.5 g,180 mmol), and DMF (300 mL). The mixture was stirred at room temperature for 24 h and filtered. The filtrate was diluted with ethyl acetate (1200 mL), and the organic layer was separated. The organic layer was washed three times with water, then dried with magnesium sulfate, and filtered. The filtrate was evaporated to afford yellowish crystals, which recrystallized from methanol/ethyl acetate to yield 18.33 g (61%) of off-white crystals; mp 120.0−121.2 °C. IR (KBr, cm^{-1}): 3446, 3072, 2971, 2877, 2451, 1904, 1610 (NO_2), 1344 (NO_2), 1249 (ether). NMR (DMSO-d_6, δ in ppm) 1.70 (s, 6H, CH_3), 7.11−7.14 (m, 8H, Ar−H), 7.35−7.38 (m, 4H, Ar−H), 8.23−8.27 (m, 4H, Ar−H). MS (m/z) 470 (M^+). Anal. Calcd for $C_{27}H_{23}N_2O_6$: C, 68.80%; H, 4.89%; N, 6.01%. Found: C, 69.52%; H, 4.76%; N, 5.70%.

2,2-Bis[4-(4-aminophenoxy)phenyl]propane (4). 2,2-Bis[4-(4-nitrophenoxy)phenyl]propane (**3**; 5.0 g, 10.6 mmol) dissolved in ethyl acetate (100 mL) and palladium on activated carbon (0.30 g) was placed in a hydrogenation bottle. The bottle was tightly secured on a Parr hydrogenation apparatus, flushed four times with hydrogen, and pressurized to 55 psi. After the mixture had been agitated at room temperature for 24 h under the hydrogen pressure of 55 psi, it was filtered through Celite. The filter cake was washed with ethyl acetate, and then the filtrate was evaporated to dryness on a rotary evaporator to afford 4.214 g (95%) of off-white crystals; mp 126.5−127.5 °C. IR (KBr, cm^{-1}): 3423, 3402, 3333, 3235 (amine), 3038, 2964, 2869, 1879, 1733, 1610, 1498, 1222 (ether), 872. ^{1}H NMR (DMSO-d_6, δ in ppm): 1.55 (s, 6H, CH_3), 4.94 (s, 4H, NH_2), 6.55−6.71(m, 4H, Ar−H), 6.71−6.77 (m, 8H, Ar−H), 7.11−7.13 (m, 4H, Ar−H). Anal. Calcd for $C_{27}H_{26}N_2O_2$: C, 79.00%, H, 6.38%, N, 6.82%, Found: C, 78.27%, H, 6.65%, N, 6.45%.

2,2-Bis{4-[4-(4-acetamidophenyldiazenyl)phenoxy]phenyl}-propane (6). 2,2-Bis[4-(4-aminophenoxy)phenyl]propane (**4**; 0.821 g, 2.00 mmol), *N*-(4-nitrosophenyl)acetamide (5; 1.312 g, 8 mmol), and acetic acid (40 mL) were charged into a 150 mL round-bottomed flask equipped with a magnetic stir bar. The mixture was stirred at room temperature for 48 h. The mixture at first turned into a greenish solution, and then yellow particles started to precipitate out of the solution. The mixture was diluted by deionized water (100 mL). Solids were collected and washed with water (500 mL) followed by of ethanol (200 mL) to remove most of the unreacted nitroso reagent. The raw product was slurried in hot ethanol (50 mL) and filtered after being cooled to room temperature twice to give 0.91 g (65%) of yellow solids; mp 267.2−269.1 °C (dec.). IR (KBr, cm^{-1}): 3320 (NHCO), 3062, 2964, 1674 (C═O), 1594, 1503, 1489, 1238, 1115, 849. MS (m/e): 702 (M^+). ^{1}H NMR (d_6-DMSO, δ in ppm): 1.67 (s, 6H, COCH_3), 2.08 (s, 6H, CCH_3) 7.05−7.13 (dd, 8H, Ar−H), 7.30−7.32 (d, 4H, Ar−H), 7.77−7.88 (m, 12H, Ar−H), 10.27 (s, 2H, NHCO). ^{13}C NMR (d_6-DMSO, δ in ppm): 24.12, 30.57, 41.84, 118.23, 119.08, 123.43, 124.36, 128.26, 142.10, 146.16, 147.37, 147.65, 153.32, 159.37, 168.72. Anal. Calcd for $C_{43}H_{38}N_6O_4$: C, 73.49%, H, 5.45%, N, 11.96%, Found: C, 73.33%, H, 5.37%, N, 11.70%.

2,2-Bis{4-[4-(4-aminophenyldiazenyl)phenoxy]phenyl}-propane (7a). To a 500 mL round-bottomed flask with a stir bar and a condenser, 2,2-bis{4-[4-(4-acetamidophenyldiazenyl)phenoxy]-phenyl}propane (**6**; 5.00 g, 7.11 mmol), 6 M HCl (200 mL), and 95% ethanol (20 mL) were charged and heated to 105 °C for 48 h. After it was allowed to cool to room temperature, water (600 mL) was added. The resulting red solid was collected by filtration and washed with 1 N sodium hydroxide solution, followed by deionized water (300 mL). After being air-dried, the crude product was purified by column chromatography (silica gel, ethyl acetate as eluent). The solvent was removed by a rotary evaporator to afford 2.95 g (67%) of orange red solid; mp 162.0−163.1 °C. IR (KBr, cm^{-1}): 3467, 3381 (NH_2), 3036, 2964, 1619, 1598, 1505, 1489, 1238, 1145, 834. MS (m/e): 618 (M^+). ^{1}H NMR (d_6-DMSO, δ in ppm): 1.66 (s, 6H, CCH_3), 6.03 (s, 4H, NH_2), 6.64−6.66 (d, 4H, Ar−H), 7.01−7.03 (d, 4H, Ar−H), 7.07−7.09 (d, 4H, Ar−H), 7.28−7.30 (d, 4H, Ar−H), 7.61−7.63 (d, 4H, Ar−H), 7.75−7.77 (d, 4H, Ar−H).^{13}C NMR (d_6-DMSO, δ in ppm): 30.54, 41.73, 113.31, 118.41, 118.64, 123.45, 124.85, 128.12, 142.72, 145.77, 148.15, 152.49, 153.73, 157.87. Anal. Calcd for $C_{39}H_{34}N_6O_2$: C, 75.71%; H, 5.54%; N, 13.58%. Found: C, 75.62%; H, 5.39%; N, 13.48%.

dx.doi.org/10.1021/ma402178z | Macromolecules 2014, 47, 659−667

Model Compound Synthesis (2,2-Bis{4-[4-(4-phthalimidophenyldiazenyl)phenoxy]phenyl}propane, 7b). Into a 50 mL three-necked flask equipped with a magnetic stir bar and nitrogen inlet and outlet were placed 2,2-bis{4-[4-(4-aminophenyldiazenyl)phenoxy]phenyl}propane (0.33 g, 0.53 mmol), phthalic anhydride (0.24 g, 1.6 mmol), and acetic acid (10 mL). The mixture was stirred under refluxing 14 h and allowed to cool to room temperature. The precipitate was collected by filtration and dried in oven to afford 0.96 g (81%) of orange powder; mp 247.7−249.7 °C. IR (KBr, cm^{-1}): 3063, 2964, 1788, 1720, 1592, 1493, 1386, 1256, 1114, 841, 715. MS (*m*/*e*): 878.29 (M^+). Anal. Calcd for $C_{55}H_{38}N_6O_6$: C, 75.16%; H, 4.36%; N, 9.56%. Found: C, %; H, %; N, %. ^1H NMR (d_6-DMSO, δ in ppm): 1.69 (s, 6H, CCH_3), 7.08−7.10 (d, 4H, Ar−***H***), 7.16−7.18 (d, 4H, Ar−***H***), 7.33−7.35 (d, 4H, Ar−***H***), 7.67−7.70 (d, 4H, Ar−***H***), 7.91−8.02 (m, 16H, Ar−***H***).

Procedure for the Preparation of PMDA Polyimide (10a, AzoBPA-PMDA). 2,2-Bis{4-[4-(4-aminophenyldiazenyl)phenoxy]-phenyl}propane (**7a**; 0.3184 g, 0.5246 mmol) and DMAc (4 mL) were added to a 25 mL three-necked flask equipped with a magnetic stirrer, nitrogen inlet, and outlet and stirred under dry nitrogen at room temperature for 30 min. PMDA (**8a**; 0.1122 g, 0.5246 mmol) was then charged. The dark red solution was agitated at room temperature for 24 h to afford a viscous poly(amic acid) solution. This solution was diluted with DMAc (3 mL), poured into a glass dish, followed by vacuum evaporation of DMAc at 50 °C, and heat-treated at 100 °C/2 h, 150 °C/2 h, 175 °C/1 h, 200 °C/2 h, 250 °C/1 h, and 300 °C/1 h to form imidized polymers. The film thickness was approximately 20−100 μm. FT-IR (KBr, cm^{-1}): 3049 (Ar−H), 2965 (CH_3), 1777, 1719 (imide), 1587, 1488, 1356, 1232, 1169, 1113, 1080, 1012, 821, 722, 546.

Procedure for the Preparation of BPDA Polyimide (10b, AzoBPA-BPDA). The OPDA polyimide (**10b**) was prepared from 2,2-bis{4-[4-(4-aminophenyldiazenyl)phenoxy]phenyl}propane (**7a**; 0.2849 g, 0.461 mmol), OPDA (**8b**; 0.1355 g, 0.461 mmol), and DMAc (5.0 mL) using the same procedures as **10a** to form imidized polymers. The film thickness was approximately 20−100 μm. FT-IR (KBr, cm^{-1}): 3053 (Ar−H), 2964 (CH_3), 1775, 1714 (imide), 1588, 1489, 1417, 1359, 1233, 1077, 1012, 832, 736, 548.

Procedure for the Preparation of BTDA Polyimide (10c, AzoBPA-BTDA). The BTDA polyimide (**10c**) was prepared from 2,2-bis{4-[4-(4-aminophenyldiazenyl)phenoxy]phenyl}propane (**7a**; 0.3583 g, 0.579 mmol), BTDA (**8c**; 0.1866 g, 0.679 mmol), and DMAc (5.0 mL) using the same procedures as **10a** to form imidized polymers. The film thickness was approximately 20−100 μm. FT-IR (KBr, cm^{-1}): 3054 (Ar−H), 2964 (CH_3), 1779, 1714 (imide), 1588, 1489, 1361, 1235, 1080, 1012, 831, 714, 549.

Procedure for the Preparation of 6FDA Polyimide (10d, AzoBPA-6FDA). The 6FDA polyimide (**10d**) was prepared from 2,2-bis{4-[4-(4-aminophenyldiazenyl)phenoxy]phenyl}propane (**7a**; 0.5087 g, 0.822 mmol), 6FDA (**8d**; 0.3652 g, 0.822 mmol), and DMAc (5.5 mL) using the same procedures as **10a** to form imidized polymers. The film thickness was approximately 20−100 μm. FT-IR (KBr, cm^{-1}): 3052 (Ar−H), 2966 (CH_3), 1785, 1722 (imide), 1589, 1489, 1411, 1232, 1207, 1191, 1138, 1080, 1012, 834, 720, 548.

Procedure for the Preparation of OPDA Polyimide (10e, AzoBPA-OPDA). The OPDA polyimide (**10e**) was prepared from 2,2-bis{4-[4-(4-aminophenyldiazenyl)phenoxy]phenyl}propane (**7a**; 0.4770 g, 0.771 mmol), OPDA (**8e**; 0.2392 g, 0.771 mmol), and DMAc (5.0 mL) using the same procedures as **10a** to form imidized polymers. The film thickness was approximately 20−100 μm. FT-IR (KBr, cm^{-1}): 3056 (Ar−H), 2964 (CH_3), 1778, 1714 (imide), 1589, 1489, 1230, 1078, 1012, 834, 705, 549.

RESULTS AND DISCUSSION

Our prior work has demonstrated that irradiation of linear and cross-linked azobenzene-functionalized polyimides (azo-PIs) can generate considerable photogenerated stress (relative to azobenzene-functionalized liquid crystal networks, azo-LCN).[5−8,17] The goal of this work is to isolate the contribution of backbone rigidity to photomechanical effects in polymeric materials. Toward this end, a series of five azobenzene-functionalized polyimides were prepared in which the rigidity of the imide unit varies widely as a function of the dianhydride structure. The azo-PIs examined here were prepared with a new diamine containing two azobenzenes per molecule (**7a**, azoBPA-diamine). The four-step synthesis of **7a** is shown in Scheme 1. To prepare **7a**, 2,2-bis(4-hydroxyphenyl)-propane (i.e., bisphenol A, **1**) was treated with 1-fluoro-4-nitrobenzene (**2**) in the presence of potassium carbonate to yield 2,2-bis[4-(4-nitrophenoxy)phenyl]propane (**3**). **3** was then reduced to 2,2-bis[4-(4-aminophenoxy)phenyl]propane (**4**) by catalytic hydrogenation. The condensation reaction of **4** and 4-nitrosoacetanilide[35] (**5**) in acetic acid yielded **6**, a precursor containing two azobenzene units. The azoBPA-diamine monomer (**7a**) was generated after the deprotection (deacetylation) of **6** via alkaline hydrolysis. To facilitate examination of photoisomerization of the chromophore unit, the model compound diphthalimidobis-(azobenzene) **7b** was synthesized by end-capping **6** with phthalic anhydride as shown in Scheme 1. The photoisomerization of **7b** was examined in solution (Figures S1 and S2 of the Supporting Information). The two-stage synthesis of the azobenzene-containing polyimides (azoBPA-XXDA, where XX stands for the generic dianhydride with the specific chemical structure and associated code as indicated in Scheme 2) was conducted as follows: (i) a dianhydride (**8**) and azoBPA-diamine (**7a**) were dissolved temperature for 24 h to generate poly(amic acid) (PAA, **9**); (ii) the resulting PAA precursor was poured onto glass slides and cured in an oven set to 300 °C to imidize the polymer

Scheme 1. Syntheses of Bis(azobenzeneamine) Monomer (7a) and Model Compound (7b)

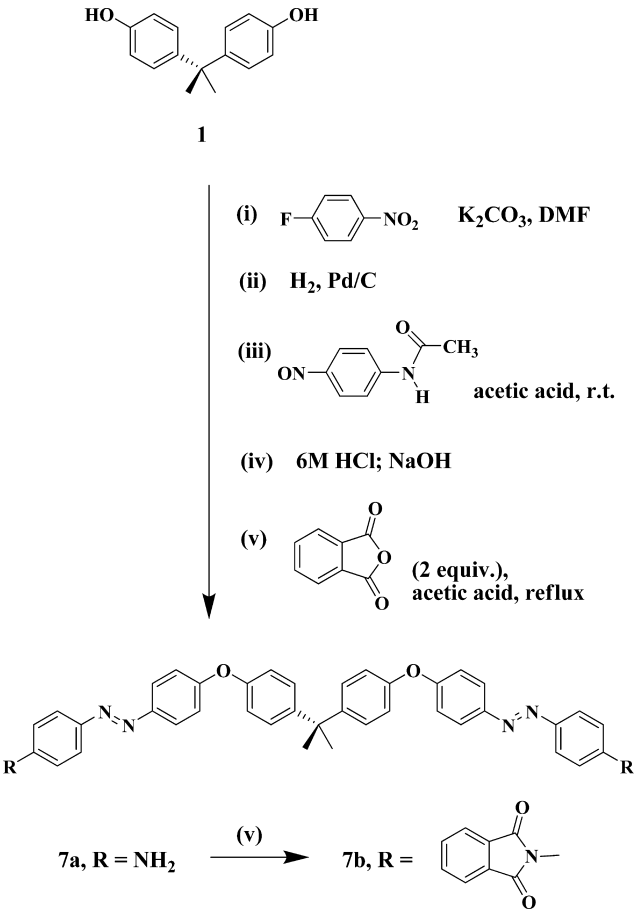

dx.doi.org/10.1021/ma402178z | *Macromolecules* 2014, 47, 659−667

Scheme 2. Synthesis of Linear Azobenzene-Containing Polyimides 10a–e

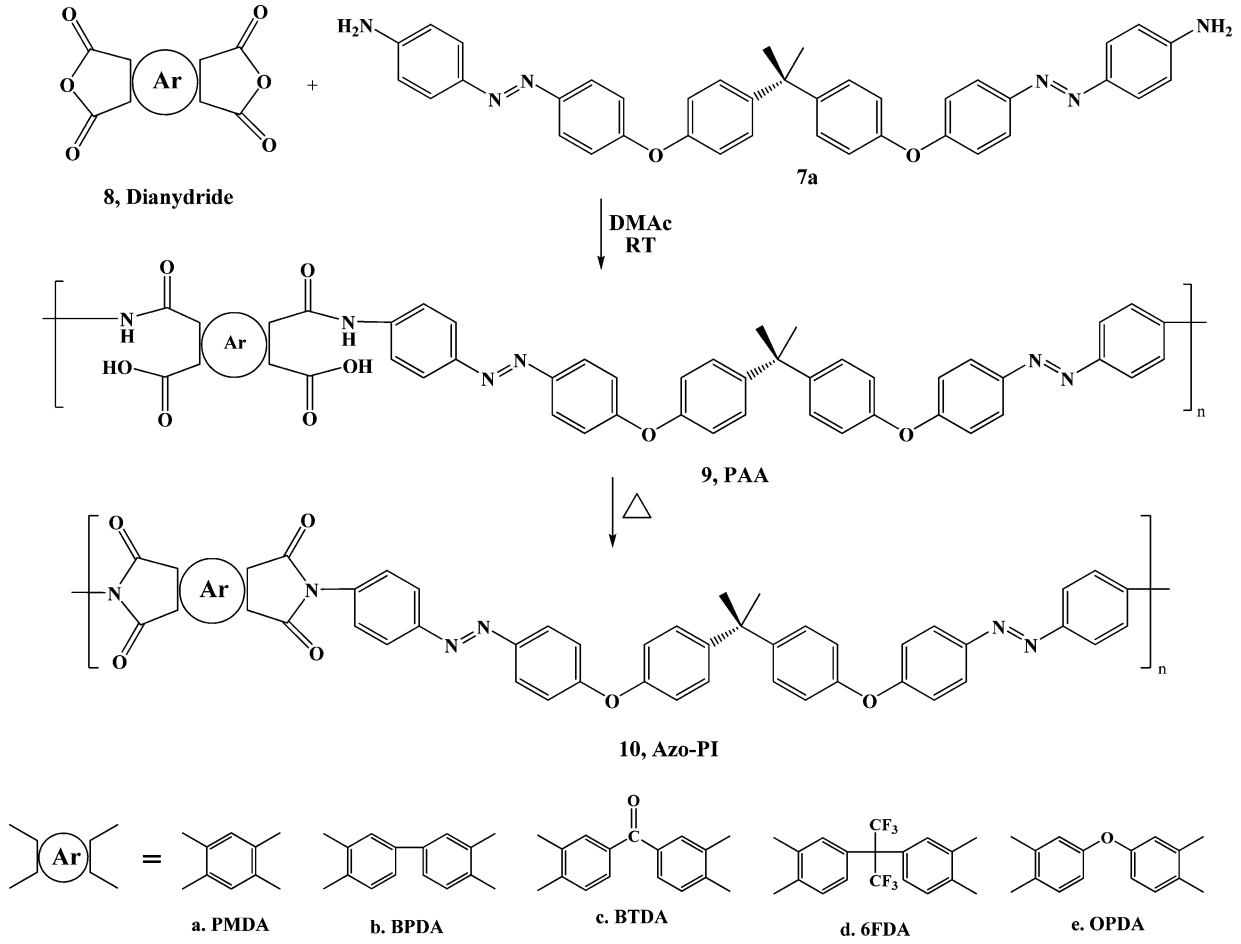

films. The formulation, density, T_g, T_d, and absorption coefficient of the materials are summarized in Table 1.

The thermomechanical properties of the azobenzene-functionalized polyimides (azo-PIs) were characterized. The glass transition temperatures (T_g) of the materials were measured by DMA from the peak of the tan δ and range from 276 to 307 °C (Table 1). The tensile properties of polyimide films were characterized by DMA with 0.01 s^{-1} Hencky strain (or true strain). The raw data are shown in Figure 1, and the values of the tensile modulus, yield stress, ultimate tensile strength, strain to failure, and toughness for the five polymers are summarized in Table 2. In the elastic regime, azoBPA-PMDA exhibited the largest tensile modulus (2.51 GPa) and azoBPA-OPDA had the lowest tensile modulus (1.34 GPa) (see Figure S5 for linear regime in stress–strain curves). AzoBPA-PMDA and azoBPA-OPDA had the largest and the lowest yield stress, respectively. After the yield point, significant strain hardening was observed only from azoBPA-PMDA. Generally, polymers showing larger strain hardening have ductile deformation and larger toughness due to strain delocalization.[36] As expected, azoBPA-PMDA had a significantly greater toughness (or energy to break) as well as extensibility (rigid–ductile) compared to other polyimides. AzoBPA-OPDA exhibits comparable toughness to azoBPA-PMDA due to the significant elongation after yield as evident in Figure 2. The large value of the strain to failure of azoBPA-OPDA is attributed to chain flexibility promoted by the rotational freedom of the ether linkage in the oxydiphthalic imide (OPDI) unit.[12]

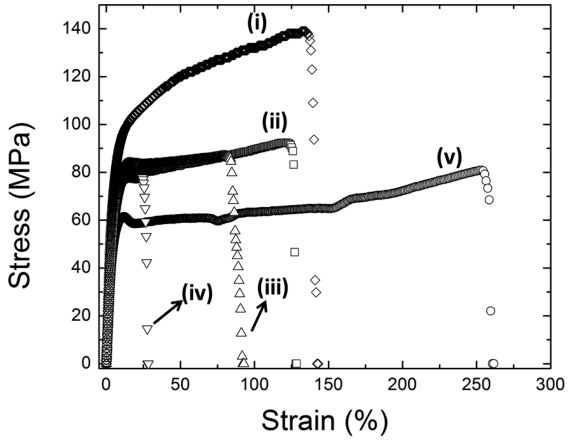

Figure 1. Representative stress–strain responses of polyimide films in uniaxial tension: (i) azoBPA-PMDA, (ii) azoBPA-BPDA, (iii) azoBPA-BTDA, (iv) azoBPA-6FDA, and (v) azoBPA-OPDA.

Classically, the conformational rigidity of a polymer can be described by the Kuhn length or persistence length.[37–40] Experimental examinations[41–43] have correlated these theoretical descriptions to measurable physical properties such as glass transition temperature[42,44] or modulus.[45] At the molecular level, the conformational rigidity of a single chain can be reasonably assumed to be dictated by the rigidity of the repeating unit. Thus, in the polyimides presented here the molecular rigidity of the repeat unit is varied by the employment of five

dx.doi.org/10.1021/ma402178z | Macromolecules 2014, 47, 659–667

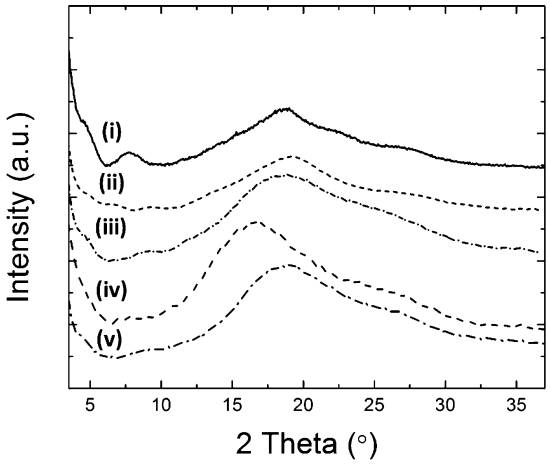

Figure 2. Wide-angle X-ray diffraction patterns of the materials examined here: (i) azoBPA-PMDA, (ii) azoBPA-BPDA, (iii) azoBPA-BTDA, (iv) azoBPA-6FDA, and (v) azoBPA-OPDA.

anhydrides of varying composition and rigidity. In the case of PMDA, BPDA, and BTDA, all of which are composed of skeletal sp^2-carbons, the rigidity can be qualitatively assessed based on the number of single C−C bonds between the two phenylene rings. Accordingly, the rigidity of the repeat unit should vary as PMDA > BPDA > BTDA. In the case of the polyimides based on 6FDA and OPDA, the rigidity will be strongly influenced by the steric limitations imparted by the sp^3-swivel moiety between the phenylene rings, and the $\rangle C(CF_3)_2$ moiety in 6FDA is expected to be more rigid than the oxygen linkage in OPDA. Thus, based on this qualitative correlation that is supported by prior literature[46] as well as the thermomechanical properties reported in Figure 1, Table 2, and the Supporting Information—the molecular rigidity of the polyimides are expected to rank as PMDA > BPDA > BTDA > 6FDA > OPDA.

The morphology of the materials was characterized with wide-angle X-ray diffraction (WAXD). As evident in Figure 2, azoBPA-OPDA, azoBPA-6FDA, and azoBPA-BTDA were completely amorphous evident in the featureless diffraction patterns of these materials. The diffraction patterns of azoBPA-PMDA and azoBPA-BPDA revealed very slight crystalline characteristics with calculated crystallinity indices of 1.5% and 0.4%, respectively. The influence of the very low crystalline content on the photomechanical response of these materials is expected to be negligible.[5]

The azobenzene chromophores in the polyimide materials examined here absorb 445 nm light, and a small portion of these chromophores reorient in the direction perpendicular to light polarization through trans−cis−trans reorientation mechanism.[47] Because of the large absorption coefficient of the materials (summarized in Table 1), light is absorbed nonuniformly across the sample thickness. The absorption gradient is then mirrored by a strain gradient which causes deflection of the film in the cantilever geometry. The magnitude of the deflections can be quantified by reporting

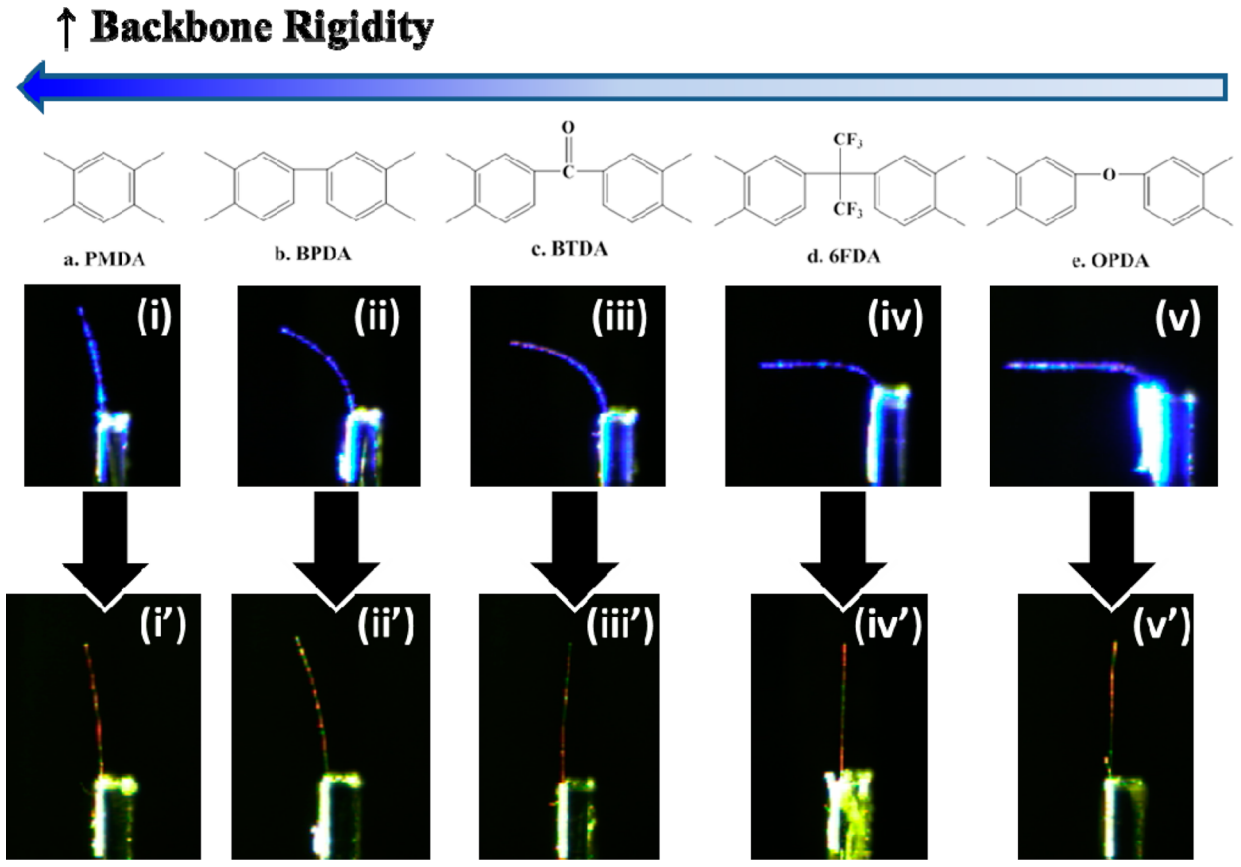

Figure 3. Photoinduced bending of cantilevers composed of (i) azoBPA-PMDA, (ii) azoBPA-BPDA, (iii) azoBPA-BTDA, (iv) azoBPA-6FDA, and (v) azoBPA-OPDA upon exposure to linearly polarized 445 nm light ($E \| x$) at 120 mW/cm^2 for 1 h. The retention or relaxation of the materials is apparent in the images of the cantilevers collected 10 days after irradiation (i′) azoBPA-PMDA, (ii′) azoBPA-BPDA, (iii′) azoBPA-BTDA, (iv′) azoBPA-6FDA, and (v′) azoBPA-OPDA.

dx.doi.org/10.1021/ma402178z | *Macromolecules* 2014, 47, 659−667

Table 1. Composition, Thermal, and Optical Properties of Polyimide Films

sample	dianhydride (mol %)	**7a** (mol %)	APB (mol %)	density (g/cm^3)	T_g[a] (°C)	$T_{d5\%}$[b] (°C) in air	$T_{d5\%}$[b] (°C) in nitrogen	$\alpha_{445\ nm}$[c] (cm^{-1})
azoBPA-PMDA	100	100	0	1.363	307	451	424	331
azoBPA-BPDA	100	100	0	1.355	302	458	427	525
azoBPA-BTDA	100	100	0	1.347	294	456	422	570
azoBPA-6FDA	100	100	0	1.339	284	474	421	723
azoBPA-OPDA	100	100	0	1.304	276	451	420	801

[a] T_g measured from the peak of tan δ (DMA) as an average value taken from four measurements. [b] Temperature at which 5% weight loss as recorded on TGA thermogram with a heating rate of 10 °C/min (raw data plotted in Figures S3 and S4, Supporting Information). [c] Measured absorption coefficient for the polyimide films at 445 nm.

Table 2. Tensile Properties of Polyimide Films

sample	tensile modulus (GPa)	yield stress (MPa)	ultimate tensile strength (MPa)	strain to failure (%)	toughness (MJ/m^3)
azoBPA-PMDA	2.51 ± 0.16	99.1 ± 8.3	147.0 ± 11.0	147.5 ± 17.9	213.7 ± 57.7
azoBPA-BPDA	1.99 ± 0.42	86.5 ± 6.6	95.5 ± 5.6	127.5 ± 18.2	121.5 ± 10.6
azoBPA-BTDA	1.66 ± 0.14	92.6 ± 12.3	94.1 ± 10.3	82.4 ± 20.9	63.5 ± 12.1
azoBPA-6FDA	1.37 ± 0.17	75.0 ± 4.7	75.1 ± 4.7	23.3 ± 4.1	19.0 ± 4.1
azoBPA-OPDA	1.34 ± 0.10	63.7 ± 3.0	81.7 ± 1.2	257.6 ± 5.8	228.4 ± 3.5

the bending angle between the mounting and tip points of the cantilever. In Figure 3, photoinduced bending (i−v) and the retention/relaxation (i′−v′) of the polyimide films were monitored in the cantilever geometry upon exposure to 445 nm light linearly polarized parallel to the long axis of the cantilever ($E\|x$) at 120 mW/cm^2 for 1 h as well as after storage of the materials in the dark (10 days), respectively. Polyimide films prepared with PMDA and BPDA (tensile modulus ≥2 GPa) had smaller magnitude of bending than the other polymers. The response of the polymers after dark storage was also dependent on the local molecular rigidity. Partial optically fixable shape memory[48] was observed in the azo-PI materials with more rigid backbone chemistries while the shape restoration in the dark was observed in azo-PI with more flexible backbones chemistries.

Photoinduced bending and unbending (relaxation) were further investigated in the materials with the most rigid backbone (azoBPA-PMDA) and contrasted to the response observed in the material with the most flexible backbone (azoBPA-OPDA). As summarized in Figure 4a, the magnitude of the photomechanical response (derived from cantilever bending) was measured both during and immediately after irradiation. Both polyimides reached near-equilibrium bending angle within 30 min. The bending angle was then monitored over the course of 10 days after light was removed. As evident in Figure 4a, the photogenerated strain in azoBPA-OPDA relaxed, and the sample fully recovered to the original vertical position. Interestingly, after the irradiation of the azoBPA-PMDA cantilever was taken away, a slight reduction in bending was observed, but a nonzero bending angle was retained over the course of 10 days.

The photomechanical responses of azoBPA-PMDA and azoBPA-OPDA were measured by DMA (Figure 4b) with concomitant irradiation of linearly polarized ($E\|x$) blue light. Irradiation of the materials in these conditions generated contractile stress, which was measured as positive stress by DMA in tension. The photogenerated stress measured by the DMA also reached equilibrium in 30 min for both polyimides. Irradiation of azoBPA-PMDA generated larger magnitude of stress. After the removal of light, ca. 250 kPa of stress is retained within azoBPA-PMDA while full stress relaxation was observed within azoBPA-OPDA.[49] We attribute the negative stress sign after the relaxation to the convolution of prestrain, photoinduced creep, and photosoftening.[50,51]

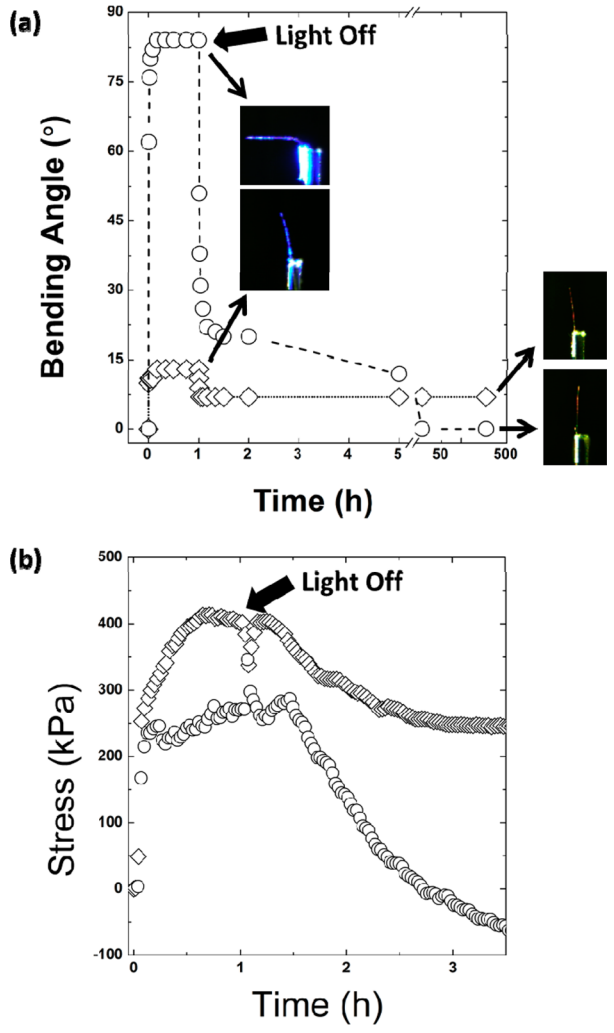

Figure 4. Temporal response of azoBPA-PMDA (◇) and azoBPA-OPDA (○) in (a) cantilever bending and (b) tension upon exposure to linearly polarized ($E\|x$) 445 nm light.

dx.doi.org/10.1021/ma402178z | *Macromolecules* 2014, 47, 659−667

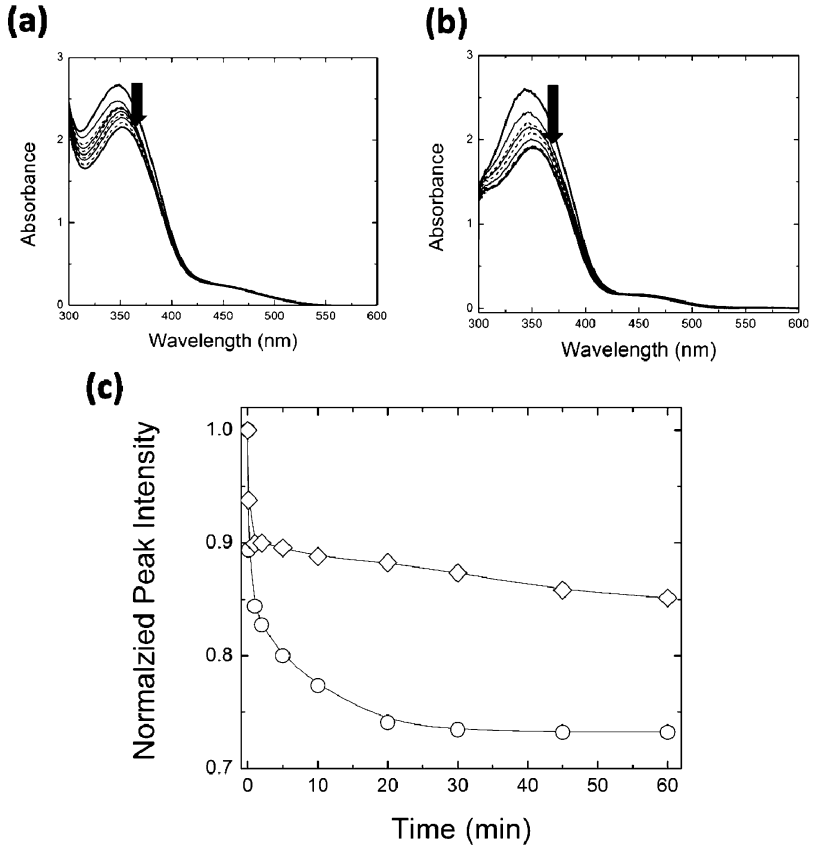

Figure 5. Absorption spectra of (a) azoBPA-PMDA and (b) azoBPA-OPDA upon the irradiation of linear polarized (*E*||*x*) 445 nm light exposure at 60 mW/cm^2 for the duration of 1 h. (c) Normalized absorption peak intensity of azoBPA-PMDA (◇) and azoBPA-OPDA (○) as a function of time.

The photochemical responses of azobenzene materials are known to be strongly impacted by the local molecular environment. In polymers, the isomerization and/or reorientation of the azobenzene chromophores requires sufficient free volume. Density measurements, summarized in Table 1, indicate that azoBPA-PMDA has a higher density (and likely reduced free volume) than azoBPA-OPDA. Less clear in the prior literature is the influence of the rigidity of the polymer backbone on the extent of azobenzene isomerization. To isolate the impact of backbone rigidity on the photochemical response of the materials examined here, absorption spectra were collected for azoBPA-PMDA (most rigid backbone chemistry) and azoBPA-OPDA (least rigid backbone chemistry) during irradiation. The absorbance spectra (normalized to account for slight differences in sample thickness) were collected from thin, spin-cast polyimide films (on glass substrates) before and during 60 min of exposure to linearly polarized (*E*||*x*) 445 nm light at 60 mW/cm^2. As illustrated in the data in Figure 5a–c, the less rigid and dense materials (azoBPA-OPDA) exhibits a considerable increase in the photochemical response, as indicated by the reduction in absorbance of the material at 365 nm upon irradiation with 445 nm light.

As discussed, the photomechanical effects in polymeric materials are interesting from the perspective of applications relating to shape change or actuation. The goal of this study was to elucidate the contribution of polymer backbone rigidity to photomechanical effects in azobenzene-functionalized polyimides examined here.[52] As discussed earlier, the rigidity of the backbone can be strongly correlated to modulus. Thus, the photomechanical response of the materials examined here is summarized in Figure 6 for both cantilever bending and tensile experiments as a function of modulus. The photomechanical response when visualized in cantilever bending experiments decreases as modulus increased. The opposite trend is observed

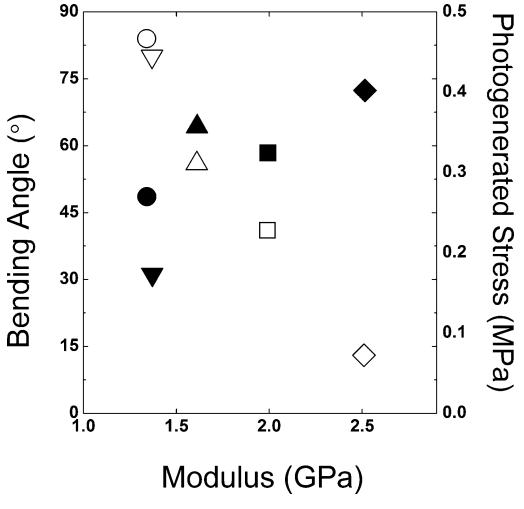

Figure 6. Dependence of the photomechanical response measured as cantilever bending (open symbols) and photogenerated stress (filled symbols).

in the tensile experiment. These two experiments are measuring sticks for the potential utility of these materials—shape change (cantilever bending) or actuation (tensile experiment). From Figure 6 it is clear that in applications relating to shape change

dx.doi.org/10.1021/ma402178z | *Macromolecules* 2014, 47, 659–667

more flexible backbone chemistries (lower modulus) allow the identical input energy stimulus to be transduced into a larger deflection. However, in the employment of these materials in applications in actuation (leveraging appropriate mechanical design), the more rigid (higher modulus) materials are able to more effectively and efficiently translate the photogenerated stress to potentially generate much larger force. Thus, future implementations of these materials as energy transducers in mechanical designs should select the appropriate backbone chemistry to facilitate the optimal output desired.

CONCLUSIONS

A new diamine (azoBPA-diamine) was synthesized and subsequently polymerized with five selected dianhydrides to prepare a series of heat-resistant (high degradation temperature and T_g ranging from 276 to 307 °C) and photoresponsive linear polyimides. Morphology characterization indicated that all the polyimides were amorphous or contained only a small amount of crystallinity which had negligible impact in photoinduced deformation. The rigidity of the polymer backbone (controlled by the dianhydride subunit) directly affected the mechanical properties and photomechanical response both during and after irradiation with 445 nm light. Irradiation of polyimides prepared with more rigid backbone chemistry was shown to generate comparatively small deflections in cantilever experiments and comparatively large photogenerated stresses in tensile experiments. Conversely, irradiation of polyimides with more flexible backbone chemistries was shown to generate comparatively large deflections in cantilever experiments and comparatively reduced photogenerated stresses in tensile experiments. Interestingly, shape memory (stress retention) was observed in polyimides with more rigid backbone chemistries while shape recovery (stress relaxation) was observed in the polyimides with more flexible backbone chemistries. These results attest to the importance of molecular engineering the polymer structure to tailor a material for specific and optimized photomechanical outputs.

ASSOCIATED CONTENT

Supporting Information

Figures S1–S5. This material is available free of charge via the Internet at http://pubs.acs.org.

AUTHOR INFORMATION

Corresponding Authors

*E-mail Timothy.White.24@us.af.mil, Tel 937-255-9551 (T.J.W.).

*E-mail Loon.Tan@us.af.mil, Tel 937-255-9153 (L.-S.T.).

Author Contributions

D.H.W. and J.J.W. contributed equally to this work.

Notes

The authors declare no competing financial interest.

D.H.W.: Also with UES Inc.

J.J.W. and K.M.L.: Also with Azimuth Inc.

ACKNOWLEDGMENTS

This work was completed at the Air Force Research Laboratory (AFRL) with funding provided by the Materials and Manufacturing Directorate as well as Air Force Office of Scientific Research. We are grateful to Marlene Houtz (University of Dayton Research Institute) for TGA and DMA data.

REFERENCES

(1) Lovrien, R. *Proc. Natl. Acad. Sci. U. S. A.* **1967**, *57* (2), 236–42.

(2) McConney, M. E.; Martinez, A.; Tondiglia, V. P.; Lee, K. M.; Langley, D.; Smalyukh, I. I.; White, T. J. *Adv. Mater.* **2013**, in press.

(3) de Haan, L. T.; Sánchez-Somolinos, C.; Bastiaansen, C. M. W.; Schenning, A. P. H. J.; Broer, D. J. *Angew. Chem., Int. Ed.* **2012**, *51* (50), 12469–12472.

(4) Lee, K. M.; Bunning, T. J.; White, T. J. *Adv. Mater.* **2012**, *24* (21), 2839–2843.

(5) Lee, K. M.; Wang, D. H.; Koerner, H.; Vaia, R. A.; Tan, L. S.; White, T. J. *Angew. Chem., Int. Ed.* **2012**, *51* (17), 4117–4121.

(6) Wang, D. H.; Lee, K. M.; Yu, Z. N.; Koerner, H.; Vaia, R. A.; White, T. J.; Tan, L. S. *Macromolecules* **2011**, *44* (10), 3840–3846.

(7) Lee, K. M.; Wang, D. H.; Koerner, H.; Vaia, R. A.; Tan, L. S.; White, T. J. *Macromol. Chem. Phys.* **2013**, *214* (11), 1189–1194.

(8) Wang, D. H.; Lee, K. M.; Koerner, H.; Yu, Z. N.; Vaia, R. A.; White, T. J.; Tan, L. S. *Macromol. Mater. Eng.* **2012**, *297* (12), 1167–1174.

(9) Wilson, D. S.; Stenzenberger, H. D.; Hergenrother, P. M. *Polyimides.* Chapman and Hall: New York, 1990, 1–78.

(10) Abadie, M. J. M.; Sillion, B. *Polyimides and Other High-Temperature Polymers*: Elsevier: Amsterdam, 1991; pp 1–18.

(11) Sroog, C. E. *Prog. Polym. Sci.* **1991**, *16* (4), 561–694.

(12) Usami, K.; Sakamoto, K.; Tamura, N.; Sugimura, A. *Thin Solid Films* **2009**, *518* (2), 729–734.

(13) Park, B.; Jung, Y.; Choi, H. H.; Hwang, H. K.; Kim, Y.; Lee, S.; Jang, S. H.; Kakimoto, M.; Takezoe, H. *Jpn. J. Appl. Phys., Part 1: Regul. Pap. Short Notes Rev. Pap.* **1998**, *37* (10), 5663–5668.

(14) Chigrinov, V. G. K., Kozenkov, V. M.; Kwok, H. S. *Photoalignment of Liquid Crystalline Materials: Physics and Applications* 2008, John Wiley & Sons, Chichester, UK.

(15) Koshiba, Y.; Yamamoto, M.; Kinashi, K.; Misaki, M.; Ishida, K.; Oguchi, Y.; Ueda, Y. *Thin Solid Films* **2009**, *518* (2), 805–809.

(16) Delaire, J. A.; Nakatani, K. *Chem. Rev.* **2000**, *100* (5), 1817–1845.

(17) Lee, K. M.; Koerner, H.; Wang, D. H.; Tan, L. S.; White, T. J.; Vaia, R. A. *Macromolecules* **2012**, *45* (18), 7527–7534.

(18) Agolini, F.; Gay, F. P. *Macromolecules* **1970**, *3* (3), 349–351.

(19) Jin, Y. H.; Paris, S. I. M.; Rack, J. J. *Adv. Mater.* **2011**, *23* (37), 4312–4317.

(20) Uğur, G.; Chang, J.; Xiang, S.; Lin, L.; Lu, J. *Adv. Mater.* **2012**, *24* (20), 2685–2690.

(21) Kloxin, C. J.; Scott, T. F.; Park, H. Y.; Bowman, C. N. *Adv. Mater.* **2011**, *23* (17), 1977–1981.

(22) Terao, F.; Morimoto, M.; Irie, M. *Angew. Chem., Int. Ed.* **2012**, *51* (4), 901–904.

(23) Naumov, P.; Kowalik, J.; Solntsev, K. M.; Baldridge, A.; Moon, J. S.; Kranz, C.; Tolbert, L. M. *J. Am. Chem. Soc.* **2010**, *132* (16), 5845–5857.

(24) Bushuyev, O. S.; Singleton, T. A.; Barrett, C. J. *Adv. Mater.* **2013**, *25* (12), 1796–1800.

(25) White, T. J.; Tabiryan, N. V.; Serak, S. V.; Hrozhyk, U. A.; Tondiglia, V. P.; Koerner, H.; Vaia, R. A.; Bunning, T. J. *Soft Matter* **2008**, *4* (9), 1796–1798.

(26) Warner, M.; Mahadevan, L. *Phys. Rev. Lett.* **2004**, *92* (13), 134302/1–134302/4.

(27) Corbett, D.; Warner, M. *Phys. Rev. Lett.* **2007**, *99* (17), 174302/1–174302/4.

(28) Corbett, D.; Warner, M. *Phys. Rev. E: Stat., Nonlinear, Soft Matter Phys.* **2008**, *77* (5–1), 051710/1–051710/11.

(29) Corbett, D.; Warner, M. *Phys. Rev. E: Stat., Nonlinear, Soft Matter Phys.* **2008**, *78* (6–1), 061701/1–061701/13.

(30) van Oosten, C. L.; Corbett, D.; Davies, D.; Warner, M.; Bastiaansen, C. W. M.; Broer, D. J. *Macromolecules* **2008**, *41* (22), 8592–8596.

(31) Warner, M.; Modes, C. D.; Corbett, D. *Proc. R. Soc. London, A* **2010**, *466* (2122), 2975–2989.

(32) Toshchevikov, V. P.; Saphiannikova, M.; Heinrich, G. *J. Chem. Phys.* **2012**, *137* (2), 024903.

(33) Toshchevikov, V.; Saphiannikova, M.; Heinrich, G. *J. Phys. Chem. B* **2011**, *116* (3), 913−924.
(34) Toshchevikov, V.; Saphiannikova, M.; Heinrich, G. *J. Phys. Chem. B* **2009**, *113* (15), 5032−5045.
(35) Cain, J. C. *J. Chem. Soc., Trans.* **1908**, *93*, 681−684.
(36) Hoy, R. S.; Robbins, M. O. *J. Polym. Sci., Part B: Polym. Phys.* **2006**, *44* (24), 3487−3500.
(37) Erman, B.; Flory, P. J.; Hummel, J. P. *Macromolecules* **1980**, *13* (3), 484−91.
(38) Sperling, L. H *Introduction to Physical Polymer Science*, 4th ed., Wiley-Interscience, New York, 2006; p 212−213.
(39) Rubinstein, M.; Colby, R. H. *Polymer Physics*; Oxford University Press: Oxford, 2003; p 454.
(40) Doi, M.; Edwards, S. F. *The Theory of Polymer Dynamics*; Clarendon: Oxford, 1986; p 11.
(41) Bacosca, I.; Hamciuc, E.; Bruma, M.; Ronova, I. A. J. *Iranian Chem. Soc.* **2012**, *9* (6), 901−910.
(42) Hamciuc, E.; Hamciuc, C.; Ronova, I. A. *Rev. Roum. Chim.* **2012**, *57* (4−5), 407−413.
(43) Abadie, M. J. M. *High Performance Polymers - Polyimides Based - From Chemistry to Applications*; InTech: Rijeka, Croatia, 2012; p 7.
(44) Rusu, R. D.; Damaceanu, M. D.; Bruma, M.; Ronova, I. A. *Iran. Polym. J.* **2011**, *20* (1), 29−40.
(45) Gray, E. W.; Winsor, P. A. *Liquid Crystals and Plastic Crystals*; Ellis Horwood: Chichester, 1974; Vol. *2*, pp 231−235.
(46) Ree, M.; Kim, K.; Woo, S. H.; Chang, H. J. *J. Appl. Phys.* **1997**, *81* (2), 698−708.
(47) Lee, K. M.; Tabiryan, N. V.; Bunning, T. J.; White, T. J. *J. Mater. Chem.* **2012**, *22* (2), 691−698.
(48) Mol, G. N.; Harris, K. D.; Bastiaansen, C. W. M.; Broer, D. J. *Adv. Funct. Mater.* **2005**, *15* (7), 1155−1159.
(49) Notably, after the light had been turned off, an artificial jump in measured stress was observed. This perturbation may be related to the utilization of a dynamic mode to maintain the film at a given prestrain in the tensile experiment. Upon removal of the light, the material is no longer subjecting the tensile grips to force, and accordingly the instrument adjusts to this new condition.
(50) Verploegen, E.; Soulages, J.; Kozberg, M.; Zhang, T.; McKinley, G.; Hammond, P. *Angew. Chem., Int. Ed.* **2009**, *48* (19), 3494−3498.
(51) Petr, M.; Helgeson, M. E.; Soulages, J.; McKinley, G. H.; Hammond, P. T. *Polymer* **2013**, *54* (12), 2850−2856.
(52) Because of differences in the molecular weight of the dianhydride dianhydride monomers, the molar concentration of the azobenzene diamine was varied and the corresponding increase in absorption coefficent (Table 1) is unavoidable in this study. However, based on prior reports (refs 31−33), it is expected that if the number density of azobenzene chromophores (e.g., absorption coefficient) took precedence over the contribution of the backbone rigidity—photogenerated stress measurements would decrease as a function of modulus.